Periodic mesoporous ionosilica nanoparticles for dual cancer therapy: Two-photon excitation siRNA gene silencing in cells and photodynamic therapy in zebrafish embryos

Braham Mezghrani, Lamiaa M.A. Ali, Nicolas Cubedo, Mireille Rossel, Peter Hesemann, Jean-Olivier Durand, Nadir Bettache

International Journal of Pharmaceutics
Full Length Manuscript

Periodic Mesoporous Ionosilica Nanoparticles for Dual Cancer Therapy: Two-Photon Excitation siRNA Gene Silencing in Cells and Photodynamic Therapy in Zebrafish Embryos

Braham Mezghrani[1,2,£], Lamiaa M.A. Ali[2,3,£], Nicolas Cubedo[4], Mireille Rossel[4], Peter Hesemann[1], Jean-Olivier Durand[1] and Nadir Bettache[2,*]

[1] ICGM, Univ Montpellier-CNRS-ENSCM, 1919, route de Mende, 34293 Montpellier Cedex 05, France
[2] IBMM, Univ Montpellier-CNRS-ENSCM, 1919, route de Mende, 34293 Montpellier Cedex 05, France
[3] Department of Biochemistry, Medical Research Institute, Alexandria University, 21561 Alexandria, Egypt
[4] MMDN, Inserm U1198, Univ Montpellier, Place Eugène Bataillon, 34095 Montpellier Cedex 05, France
[£] These authors contributed equally to this work
[*] Correspondence: nadir.bettache@umontpellier.fr (N.B.)

Abstract

Photodynamic therapy (PDT) and photochemical internalization (PCI) are two methods that use light to provoke cell death or disturbance of cellular membranes, respectively, v*ia* excitation of a photosensitizer and the formation of reactive oxygen species (ROS). In this context, two-photon excitation (TPE) is of high interest for PCI and/or PDT due to spatiotemporal resolution of two-photon light and deeper penetration of near-infrared light in biological tissues. Here, we report that Periodic Mesoporous Ionosilica Nanoparticles (PMINPs) containing porphyrin groups allow the complexation of pro-apoptotic siRNA. These nano-objects were incubated with MDA-MB-231 breast cancer cells, and TPE-PDT led to significant cell death. Finally, MDA-MB-231 breast cancer cells were pre-incubated with the nanoparticles and then injected in the pericardial cavity of zebrafish embryos. After 24 hours, the xenografts were irradiated with femtosecond pulsed laser and the size monitoring by imaging showed a decrease 24 h after irradiation. Pro-apoptotic siRNA was complexed with the nanoparticles and incubation with MDA-MB-231 cells did not lead to cancer cell death in dark conditions, but with two-photon irradiation, TPE-PCI was observed and a synergic effect between pro-apoptotic siRNA and TPE-PDT was noticed, leading to 90% of cancer cell death. Therefore, PMINPs represent an interesting system for nanomedicine applications.

Keywords

Periodic Mesoporous Ionosilica Nanoparticles; two-photon excitation PDT; siRNA; gene silencing; cancer therapy; zebrafish.

Graphical abstract

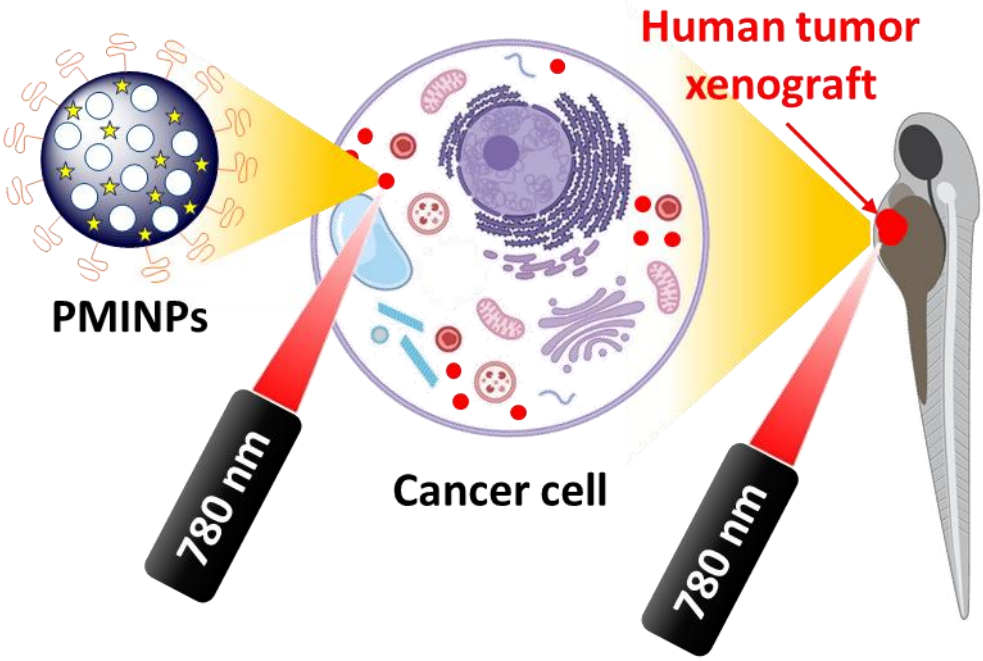

Introduction

Photodynamic therapy (PDT) (Pham et al., 2021; Sun et al., 2022) and photochemical internalization (PCI) (Jerjes et al., 2020; Soe et al., 2021) are two procedures that make use of light in order to generate singlet oxygen ($^1O_2$) and reactive oxygen species (ROS) through the excitation of a photosensitizer. The main applications of PDT are destroying small localized tumors and pathogens though the excessive production of ROS and $^1O_2$, whereas PCI is used to destabilize the cell membranes through the local production of ROS and $^1O_2$, which facilitates the internalization of biomolecules into the cytosol of cells (Ali and Gary-Bobo, 2022). It has recently been shown that the efficiencies of PDT and PCI can be greatly improved when combined with nanoparticles (Ji et al., 2022; Kwon et al., 2019; Yang et al., 2022). Commonly, one-photon excitation (OPE) light is used for PCI and PDT, but recently researchers are doing efforts to design systems that can be excited under two-photon excitation (TPE) light in near infrared (NIR) region, in order to increase the light penetration depth with less phototoxic effect (Al-Kattan et al., 2020). In the course of our work in the field of mesoporous organosilica nanoparticles (Croissant et al., 2018), we were interested in new systems based on ionosilica. Ionosilicas recently appeared as polyvalent materials for anion exchange processes (Bouchal et al., 2016; Thach et al., 2018). Here, we investigated Periodic Mesoporous Ionosilica Nanoparticles (PMINPs) for combined TPE-PDT and siRNA gene silencing in cells and TPE-PDT in zebrafish embryos. PMINPs were obtained *via* sol-gel procedures starting from cationic oligotrialkoxysilylated precursor, in the absence of any other silica source, and using anionic surfactant as porogen. We already reported that PMINPs efficiently encapsulate and deliver hydrophobic small anionic molecules such as BODIPY and anionic drugs like diclofenac or gemcitabine monophosphate into cells (Bouchal et al., 2017; Daurat et al., 2019; Mezghrani et al., 2023). Furthermore, we recently described the integration of tetrasilylated porphyrin within the walls of PMINPs (Mezghrani et al., 2021). The characterization of these nanoparticles using UV/Vis spectroscopy points towards the formation of J aggregates of porphyrins. These porphyrin-doped PMINPs allow efficient PDT and PCI of siRNA against luciferase in MDA-MB-231 breast cancer cells with visible green light. As J aggregates of porphyrins impart improved two-photon absorption properties (Biswas et al., 2012), we focused on PDT and PCI using TPE light. Here, we report our results concerning TPE-PDT and TPE-PCI of pro-apoptotic siRNA on MDA-MB-231 breast cancer cells and TPE-PDT in zebrafish embryos.

Materials and methods

PMINPs' preparation

The PMINPs synthesis was performed according to our recently described procedure from ammonium *tris*(trialkoxysilylated) precursor and *tetrakis*(trialkoxysilylated) porphyrin (Mezghrani et al., 2021).

Cell lines

Human breast cancer cell line (MDA-MB-231) was purchased from ATCC. The MDA-MB-231-LUC-RFP stable cell line expressing luciferase enzyme was obtained from AMSBIO (SC041, Abingdon, UK). Cells were grown in Dulbecco's Modified Eagle Medium Gibco™ (DMEM) supplemented with 10% fetal bovine serum (FBS) and 1% gentamycin 100 µg mL^{-1}. All cells were incubated at 37°C in humidified atmosphere with 5% CO_2.

Two-photon excitation photodynamic therapy (TPE-PDT) study

MDA-MB-231 cells were seeded into glass bottom 384-well plate (CORNING, USA), and allowed to grow for 24 hours. Then, the cells were treated with 5 and 10 µg mL^{-1} of nanoparticles for 24 hours. The used concentrations are non-toxic as previously reported (Mezghrani et al., 2021). Non-treated cells were

considered as a control. After incubation with PMINPs, the cells were exposed (or not) to pulsed titanium: sapphire laser (Chameleon Ultra, Coherent, Inc.) irradiation at two different wavelengths: 780 and 860 nm for 4.68 s (3x 1.56 s, 3 W output power). Two days later, the phototoxic effect of the nanoparticles was assessed using 3-(4,5-dimethylthiazol-2-yl)-2,5-diphenyltetrazolium bromide (MTT) cell viability assay as previously described (Al-Kattan et al., 2020). The percentage of cell viability was calculated according to the control that were not exposed to light (set as 100%).

Cellular Reactive Oxygen Species (ROS) detection

MDA-MB-231 cells were seeded into glass bottom 94-well plate (CORNING, USA) and then left to grow for 24 hours. These cells were treated with PMINPs at a concentration of 20 µg mL^{-1} for 24 hours. After the incubation period, ROS were detected using DCFDA/H_2DCFDA-Cellular ROS Assay Kit (Abcam, UK). Control cells and nanoparticles-treated cells were incubated with 20 µM of DCFDA for 45 min at 37°C, then cells were exposed (or not) to pulsed laser beam at 780 nm (3x 1.56 s, 3 W output power). After irradiation, cells were washed twice then visualized using LSM780 confocal microscope (Carl Zeiss, Germany) at 488 nm.

Dual evaluation of TPE-PDT and gene silencing using siIAP

MDA-MB-231 cells were seeded into glass bottom 384-well plate (CORNING, USA), at a density of 2000 cells *per* well for 24 hours. siIAP/PMINPs complexes were prepared in serum free cell culture medium for 30 min at 37°C using 100 nM concentration of siIAP at a weight ratio of 1/10, the weight ratio choice was based on our previous results (Mezghrani et al., 2021). Then, cells were treated (or not) with free siIAP, free PMINPs at 14 µg mL^{-1} or with siIAP/PMINPs complex for 4 hours. After that, FBS was added in each well to reach a 10% serum. After 8 hours of incubation, cells were submitted to pulsed laser irradiation at 780 nm for 4.68 s duration (3x 1.56 s, 3 W). Lipofectamine™ RNAiMAX Reagent was used as positive control transfection reagent. Results are expressed as a percentage of cell viability determined by MTT assay, and compared to the non-treated and non-irradiated control cells (set as 100%). In this case, the correct transfection of siRNA targeted against Inhibitor of Apoptosis Protein (siIAP) may increase the cell death efficiency of PDT. The obtained combination effect was then investigated using CompuSyn software (ComboSyn, Inc).

Zebrafish breeding conditions

Wild-type AB and Casper zebrafish (*Danio rerio*) strains were purchased from Zebrafish International Resource Center (ZIRC) as embryos and were raised to adulthood in circulating aquarium system inside environmentally controlled room (28°C, 80% humidity, 14 h light/10 h dark cycle), in the lab's facilities of Molecular Mechanisms in Neurodegenerative Dementia (MMDN), Inserm U1198, Montpellier University, Montpellier. Fish breeding is performed within the fish facility and platform of MMDN under the authorisation number # B-3417237 delivered by the French Department of Animal Health and Protection and Environment. Experiments with zebrafish embryos until 96 hours post-fertilization (hpf) are considered as *in vitro* studies according to the EU Directive 2010/63/EU on the protection of animals used for scientific purposes (Seisenbaeva et al., 2021).

Toxicity study of PMINPs in zebrafish embryos

Fertilized wild-type AB zebrafish eggs were collected and placed on agarose mold. A volume of 1 nL of PMINPs suspension at 0.5 or 1 mg mL^{-1} was microinjected (or not) into the fertilized eggs at one cell stage, using FemtoJet® 4x microinjector (Eppendorf, Germany). For each condition, 70 fertilized embryos were selected (n = 70). The percentages of living, deformed and dead embryos were recorded using Olympus MVX10 stereo microscope (Olympus, Japan) at 4, 24, 48 and 72 hpf.

TPE-PDT study in zebrafish embryos

MDA-MB-231-LUC-RFP cells were seeded in Nunc™ EasYFlask™ (Thermo Fisher Scientific, USA) 75 cm^2. 24 hours after seeding, cells were treated with 10 µg mL^{-1} of PMINPs for 24 h. After incubation, cells were washed thrice with PBS then trypsinized and suspended in culture medium. Cells were counted, centrifuged and then suspended in the required volume of PBS containing 10 % FBS to have a solution of 2 x 10^7 cells mL^{-1}. The suspension was kept in ice until injection. Casper zebrafish embryos at 48 hpf were used. Embryos were anesthetized with tricaine solution (168 mg L^{-1}) 10 min prior to injection. Then, embryos were placed on agarose mold for the microinjection of MDA-MB-231LUC-RFP cells previously incubated with PMINPs. Each embryo received 10 nL of cell suspension to get 200 - 400 injected cells *per* embryo in the pericardial cavity. After injection, the xenografted embryos were kept in water at 30°C. Twenty-four hours after injection, embryos were anesthetized and imaged using confocal microscopy Zeiss LSM 880 (Carl Zeiss, Germany) for the detection of cancer cell xenografts stained in red by the red fluorescent protein (RFP). Brightfield images were also acquired. Then, embryos were divided into two groups: exposed or not to irradiation, using pulsed laser at 780 nm (3x 1.56 s, 3 W). Twelve embryos were used for each condition (n = 12). Twenty-four hours later, the embryos were exposed again to imaging.

Statistical analysis

Results were presented as mean ± standard deviation (SD) of three independent experiments. The comparison between groups was analysed with Student's t-test. Differences were considered statistically significant when p values were less than 0.05. The level of significance was defined as * statistical significance difference ($p<0.05$), ** ($p<0.005$) and **** ($p<0.0001$).

Results and Discussion

The PMINPs preparation was carried out following an optimized sol-gel procedure combining tetrasilylated-porphyrin derivative to a ionosilica source (Mezghrani et al., 2021). The obtained nanoparticles showed a rod-like morphology with an average length of 108 ± 9 nm and a width of 54 ± 4 nm. The average DLS diameter of the nanoparticles was of 140 ± 23 nm as determined by DLS. Nitrogen sorption indicated that the nanoparticles display mesoporosity with a specific surface area of 1015 m^2g^{-1} and an average pore diameter of 5.1 nm. UV-Vis spectroscopy showed a red shift of the signals of the porphyrin derivative after encapsulation inside the PMINPs framework compared to the UV/Vis spectrum of the molecular porphyrin precursor. This result points towards the formation of J aggregates of the photosensitizer within the nanoparticles.

We then studied TPE-PDT with breast cancer cells (Figure 1). As shown in Figure 1a, the cell viabilities remain unchanged for untreated cells, regardless of the presence or absence of irradiation that confirms the safety of irradiation condition. For the cells that underwent nanoparticle treatment, a TPE-PDT effect was observed when using 860 nm irradiation, leading to cell death of 32 ± 4.4% and 46 ± 3.8% at concentrations of 5 and 10 µg mL^{-1} respectively. This PDT effect further increased when the treated cells were irradiated at 780 nm wavelength, thus reaching 40 ± 2.3% and 56 ± 2.0% of cell death for nanoparticle concentrations of 5 and 10 µg mL^{-1}, respectively. According to these results, the wavelength 780 nm was chosen for the following experiments.

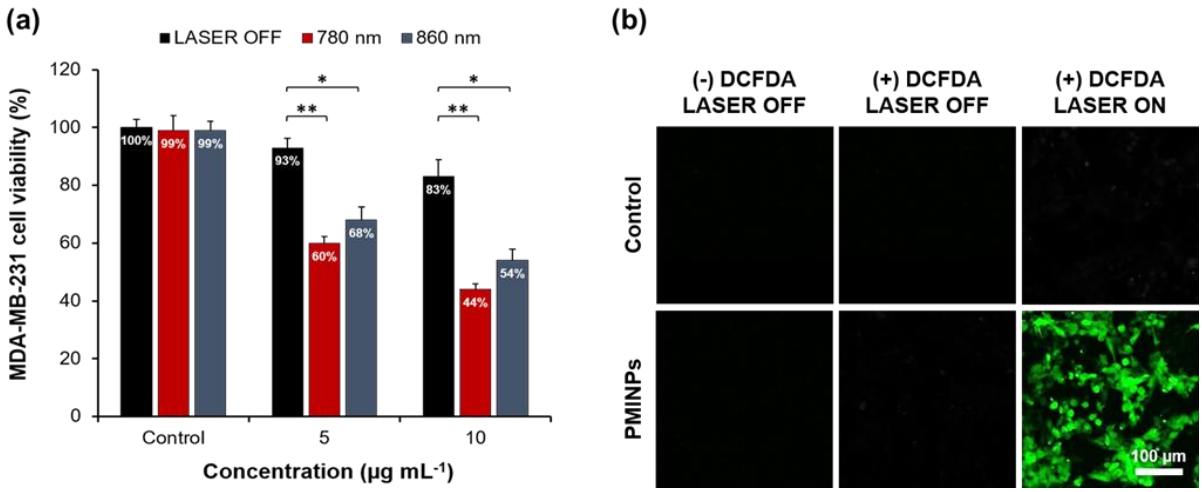

Figure 1. a) TPE-PDT studies in human breast cancer cell line (MDA-MB-231) treated with 5 or 10 µg mL^{-1} for 24 h then irradiated or not using femtosecond focused laser at two different wavelengths (780 and 860 nm, 3 x 1,56s, 3 W output). Data are presented as (mean ± SD) of three repeated experiments. **b)** Intracellular detection of ROS using DCFDA. Confocal microscopy images obtained on MDA-MB-231 cells treated (or not) with PMINPs (20 µg mL^{-1}) for 24 hours, then exposed (or not) to irradiation at 780 nm (3x 1.56 s, 3 W output) using a pulsed laser. Different conditions are used: (-) DCFDA / LASER OFF, (+) DCFDA / LASER OFF and (+) DCFDA / LASER ON.

The PDT effect was subsequently confirmed using the DCFDA kit to detect the formation of ROS that was monitored by the presence of intra-cytoplasmic green fluorescence. As shown in Figure 1b, no fluorescence was detected in the irradiated and non-irradiated controls as well as in the treated and non-irradiated cells. However, irradiation of cells treated with PMINPs revealed intense intracellular green fluorescence, indicative of photo-induced ROS production.

The *in vivo* biocompatibility of PMINPs was next examined in zebrafish eggs (Figure 2) at the unicellular stage by injecting a suspension of nanoparticles at concentrations of 0.5 and 1 mg mL^{-1}. The embryonic development of the injected (or not) eggs was monitored daily, up to 72 hours post-fertilization (hpf), by observing the appearance of malformations in the heart or tail, appearance of swelling or even death, representative images of embryos development are shown in Figure 2a. As shown in Figure 2b, no malformations were observed and viability was excellent. These results demonstrate an excellent biocompatibility of PMINPs. Indeed, at the highest concentration used of 1 mg mL^{-1}, a viability rate of 100% was observed up to 3 days post-fertilization, with a total absence of malformations in the embryos. However, at 0.5 mg mL^{-1}, we noted the death of two embryos, out of 70, at 72 hpf, corresponding to a viability of 97% at this concentration.

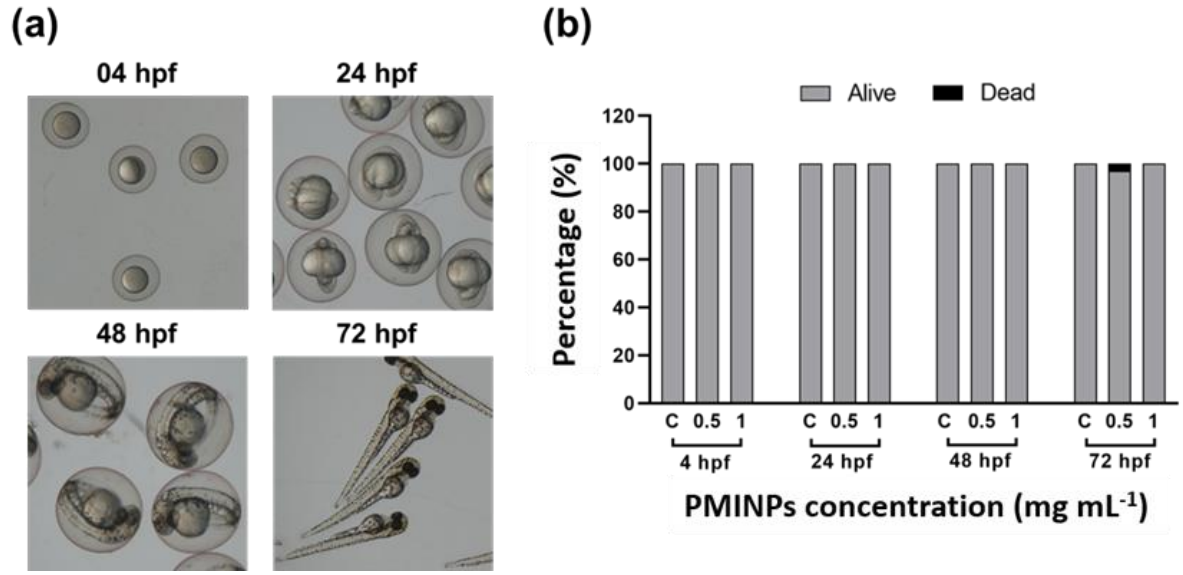

Figure 2. Study of the toxicity of PMINPs *in vivo* on fertilized zebrafish eggs, injected (or not) at single cell stage with suspensions of PMINPs at concentrations of 0.5 and 1 mg mL^{-1} and subsequently monitored daily for 3 days. **a)** Photographs represent the development of the injected eggs at different stages: 4 hpf, 24 hpf, 48 hpf and 72 hpf. **b)** A summarizing graph of the toxicity study of PMINPs in zebrafish eggs (n = 70).

We then examined TPE-PDT on zebrafish embryos xenografted in the pericardial cavity with MDA-MB-231 breast cancer cells expressing the RFP protein and pre-incubated with the PMINPs at a concentration of 10 µg mL^{-1} (Figure 3).

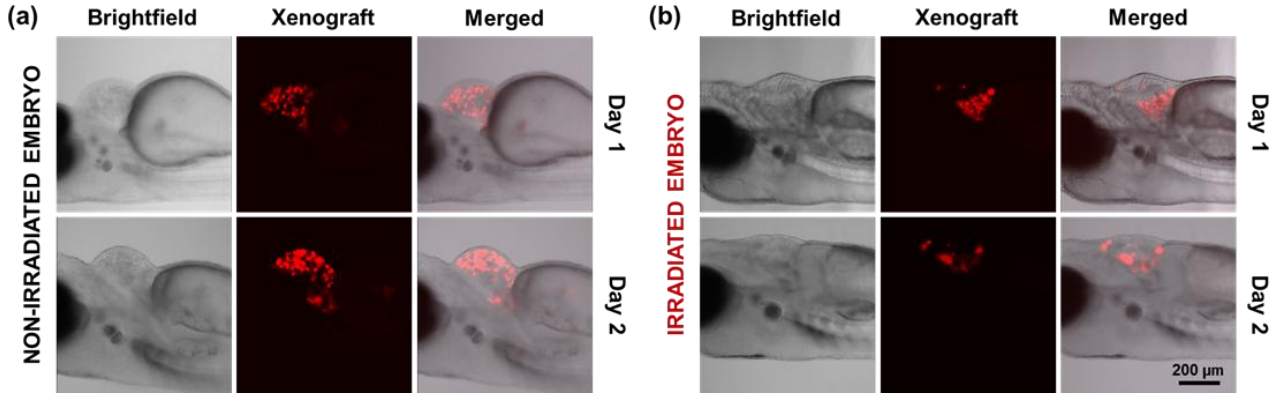

Figure 3. TPE-PDT effect of PMINPs *in vivo* in zebrafish embryos (n = 12) with xenografts of MDA-MB-231-LUC-RFP cells pre-incubated with PMINPs (10 µg mL^{-1}), irradiated **(b)**, or not **(a)**, at 780 nm (3x 1.56 s, 3 W output power). The monitoring of the xenografts labeled in red with the RFP protein was carried out through confocal microscopy. The obtained images of first day were taken 24 hours after injection, and those of the second day were taken 24 hours later after irradiation.

Two batches of zebrafish embryos xenografts of 12 individuals each (n = 12) were studied. The first batch was not irradiated, whereas the zebrafish xenografts of the second batch underwent irradiation at 780 nm (3x 1.56 s, 3 W). The embryos of batch 1 showed an increase of the red fluorescence one day after the injection of the cells in the absence of irradiation (Figure 3a), due to the growth of the tumor without irradiation. In contrast, the embryos of batch 2 (Figure 3b) showed a decrease of the red fluorescence of the xenografts 24 hours after irradiation at 780 nm (3x 1.56 s, 3 W), compared to the same embryo whose tumor was monitored before irradiation, 1 day after injection of the cancer cells.

We then investigated TPE-PCI with pro-apoptotic siRNA in MDA-MB-231 cancer cells. Pro-apoptotic siRNA (siIAP) leads to the inhibition of the production of anti-apoptotic proteins, with the activation of the apoptotic pathway, leading to cell death. For this purpose, MDA-MB-231 cells were treated (or not) with free siRNA, free PMINPs or with siIAP/PMINPs complexes for 8 hours then irradiated (or not) at 780 nm using a pulsed laser (3x 1.56 s, 3 W).

The results presented in Figure 4a show that the obtained cell viabilities with the free PMINPs and siRNA/PMINPs complexes, in the absence of irradiation, are 83 ± 2.9% and 86 ± 2.2%, respectively, and are almost identical. This high level of cell viability in cells treated with siIAP/ PMINPs can be explained by the confinement of the complex in the endo-lysosomal compartments in the absence of irradiation. Upon irradiation, a statistically significant mortality rate was observed in cells treated with free PMINPs with a value of 57 ± 0.8% due to TPE-PDT. However, the mortality rate was strongly increased when cells were treated with siIAP/PMINPs complexes and exposed to irradiation. Indeed, we observed 90 ± 0.7% cell death due to the TPE-PDT and TPE-PCI effects.

In order to determine the nature of the combination between TPE-PDT and pro-apoptotic siRNA delivery through TPE-PCI (Figures 4b and 4c), we used CompuSyn software, which determines the combination index (CI). Depending on the obtained CI value, 3 types of effects can be observed: additive effect, if CI = 1; synergistic effect, if CI < 1; antagonistic effect, if CI > 1. In the case of our study, the value of the combination index is CI = 0.43, a synergistic effect between TPE- PDT and siRNA delivery through TPE-PCI was therefore observed.

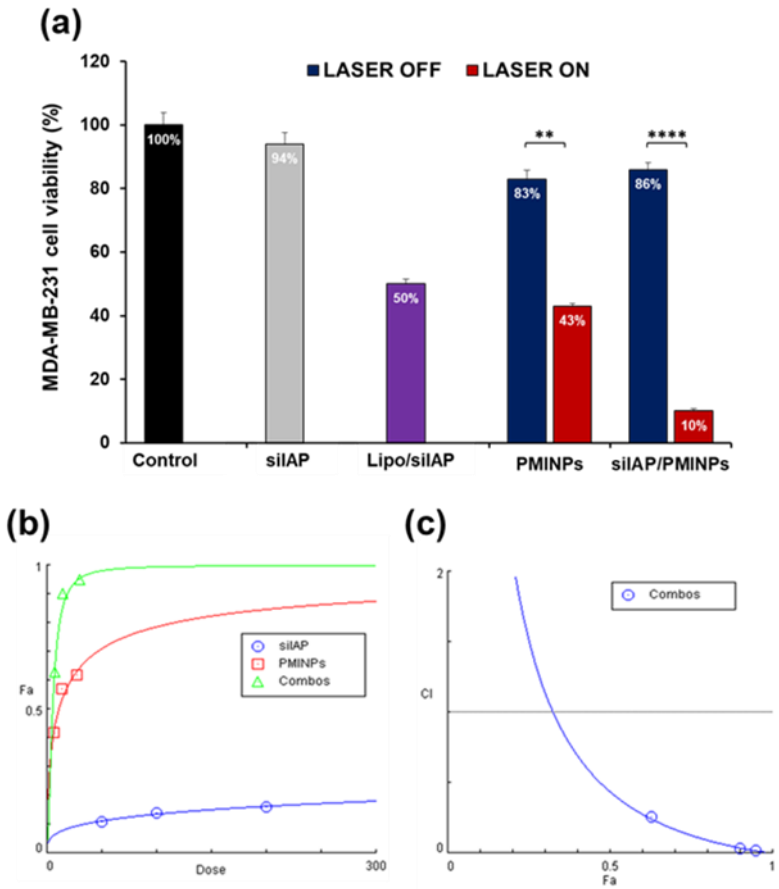

Figure 4. Study of the combination between TPE-PDT with the delivery of siIAP through TPE-PCI in MDA-MB-231 cells treated with free PMINPs, siIAP alone or with siIAP/PMINPs complexes. **a)** Cell viability of MDA-MB-231 cells treated (or not) with free PMINPs (14 µg mL^{-1}) or with siIAP/PMINPs complexes (100 nM/14 µg mL^{-1}) at a ratio of 1/10 for 8 hours, then irradiated (or not) using a focused femtosecond pulsed laser at 780 nm (3x 1.56 s, 3 W output). siIAP alone and lipofectamine/siIAP were used as transfection controls. Data are presented as (mean ± SD) of three repeated experiments. ** statistically significant difference with the same non-irradiated condition ($p < 0.005$) and ****

statistically significant difference ($p < 0.0001$). **b)** Dose-effect curves of free PMNPs, siIAP alone and the combination of both (combos). The effect represents the cell death rate. **c)** Determination of the combination index (CI) as a function of the effect obtained (Fa), CI=0.43. These two graphs (b and c) were obtained using the CompuSyn software.

Conclusion

In conclusion, we have designed PMINPs possessing J aggregates of porphyrin photosensitizer in the walls, which allowed to perform TPE-PDT on breast cancer cells and on zebrafish embryos xenografted with human breast cancer cells pre-incubated with PMINPs. The TPE-PCI on breast cancer cells with pro-apoptotic siRNA in combination with TPE-PDT was also demonstrated and showed the synergetic effect between TPE-PCI and TPE-PDT. Due to the fast development of two-photon endoscopes, the combination of these devices with PMINPs could therefore lead to new areas for nanomedicine applications.

Author contributions

BM, LMAA and NC: experimental research; JOD, PH and NB: designed project; BM, LMAA, MR, JOD, PH and NB: results analysis and project management; BM, JOD, PH and NB: funding acquisition and manuscript writing. All authors reviewed the manuscript.

Declaration of interest

The authors declare no conflicts of interest.

Acknowledgements

The authors thank the "Algerian Ministry of Higher Education and Scientific Research" for the Ph.D. grant to B.M. and the Franco-Algerian steering committee for its support. We thank Montpellier RIO Imaging platform (ANR-10-INBS-04), member of France BioImaging, for imaging facilities.

References

Al-Kattan, A., Ali, L.M.A., Daurat, M., Mattana, E., Gary-Bobo, M., 2020. Biological Assessment of Laser-Synthesized Silicon Nanoparticles Effect in Two-Photon Photodynamic Therapy on Breast Cancer MCF-7 Cells. Nanomaterials 10, https://doi.org/10.3390/nano10081462.

Ali, L.M.A., Gary-Bobo, M., 2022. Photochemical Internalization of siRNA for Cancer Therapy. Cancers 14, https://doi.org/10.3390/cancers14153597.

Biswas, S., Ahn, H.Y., Bondar, M.V., Belfield, K.D., 2012. Two-Photon Absorption Enhancement of Polymer-Templated Porphyrin-Based J-Aggregates. Langmuir 28, 1515-1522, https://doi.org/10.1021/la203883k.

Bouchal, R., Daurat, M., Gary-Bobo, M., Da Silva, A., Lesaffre, L., Aggad, D., Godefroy, A., Dieudonne, P., Charnay, C., Durand, J.-O., Hesemann, P., 2017. Biocompatible Periodic Mesoporous Ionosilica Nanoparticles with Ammonium Walls: Application to Drug Delivery. ACS Appl. Mater. Interfaces 9, 32018-32025, https://doi.org/10.1021/acsami.7b07264.

Bouchal, R., Miletto, I., Thach, U.D., Prelot, B., Berlier, G., Hesemann, P., 2016. Ionosilicas as efficient adsorbents for the separation of diclofenac and sulindac from aqueous media. New J. Chem. 40, 7620-7626, https://doi.org/10.1039/c6nj01473a.

Croissant, J.G., Zink, J.I., Raehm, L., Durand, J.O., 2018. Two-Photon-Excited Silica and Organosilica Nanoparticles for Spatiotemporal Cancer Treatment. Adv. Healthc. Mater. 7, 1701248, https://doi.org/10.1002/adhm.201701248.

Daurat, M., Rahmani, S., Bouchal, R., Akrout, A., Budimir, J., Nguyen, C., Charnay, C., Guari, Y., Richeter, S., Raehm, L., Bettache, N., Gary-Bobo, M., Durand, J.-O., Hesemann, P., 2019. Organosilica Nanoparticles for Gemcitabine Monophosphate Delivery in Cancer Cells. ChemNanoMat 5, 888-896, https://doi.org/10.1002/cnma.201900202.

Jerjes, W., Theodossiou, T.A., Hirschberg, H., Hogset, A., Weyergang, A., Selbo, P.K., Hamdoon, Z., Hopper, C., Berg, K., 2020. Photochemical Internalization for Intracellular Drug Delivery. From Basic Mechanisms to Clinical Research. Journal of Clinical Medecine 9, https://doi.org/10.3390/jcm9020528.

Ji, B., Wei, M., Yang, B., 2022. Recent advances in nanomedicines for photodynamic therapy (PDT)-driven cancer immunotherapy. Theranostics 12, 434-458, https://doi.org/10.7150/thno.67300.

Kwon, S., Ko, H., You, D.G., Kataoka, K., Park, J.H., 2019. Nanomedicines for Reactive Oxygen Species Mediated Approach: An Emerging Paradigm for Cancer Treatment. Acc. Chem. Res. 52, 1771-1782, https://doi.org/10.1021/acs.accounts.9b00136.
Mezghrani, B., Ali, L.M.A., Jakimoska, S., Cunin, F., Hesemann, P., Durand, J.O., Bettache, N., 2023. Periodic Mesoporous Ionosilica Nanoparticles for BODIPY Delivery and Photochemical Internalization of siRNA. Chempluschem 88, https://doi.org/10.1002/cplu.202300021.
Mezghrani, B., Ali, L.M.A., Richeter, S., Durand, J.-O., Hesemann, P., Bettache, N., 2021. Periodic Mesoporous Ionosilica Nanoparticles for Green Light Photodynamic Therapy and Photochemical Internalization of siRNA. ACS Appl. Mater. Interfaces 13, 29325-29339, https://doi.org/10.1021/acsami.1c05848.
Pham, T.C., Nguyen, V.-N., Choi, Y., Lee, S., Yoon, J., 2021. Recent Strategies to Develop Innovative Photosensitizers for Enhanced Photodynamic Therapy. Chem. Rev. 121, 13454-13619, https://doi.org/10.1021/acs.chemrev.1c00381.
Seisenbaeva, G.A., Ali, L.M.A., Vardanyan, A., Gary-Bobo, M., Budnyak, T.M., Kessler, V.G., Durand, J.O., 2021. Mesoporous silica adsorbents modified with amino polycarboxylate ligands-functional characteristics, health and environmental effects. J. Hazard. Mater. 406, https://doi.org/10.1016/j.jhazmat.2020.124698.
Soe, T.H., Watanabe, K., Ohtsuki, T., 2021. Photoinduced Endosomal Escape Mechanism: A View from Photochemical Internalization Mediated by CPP-Photosensitizer Conjugates. Molecules 26, https://doi.org/10.3390/molecules26010036.
Sun, N., Wen, X., Zhang, S., 2022. Strategies to Improve Photodynamic Therapy Efficacy of Metal-Free Semiconducting Conjugated Polymers. Int. J. Nanomed. 17, 247-271, https://doi.org/10.2147/IJN.S337599.
Thach, U.D., Prelot, B., Pellet-Rostaing, S., Zajac, J., Hesemann, P., 2018. Surface Properties and Chemical Constitution as Crucial Parameters for the Sorption Properties of Ionosilicas: The Case of Chromate Adsorption. ACS Appl. Nano Mater. 1, 2076-2087, https://doi.org/10.1021/acsanm.8b00020.
Yang, Y., Zeng, Z., Almatrafi, E., Huang, D., Zhang, C., Xiong, W., Cheng, M., Zhou, C., Wang, W., Song, B., Tang, X., Zeng, G., Xiao, R., Li, Z., 2022. Core-shell structured nanoparticles for photodynamic therapy-based cancer treatment and related imaging. Coord. Chem. Rev. 458, 214427, https://doi.org/10.1016/j.ccr.2022.214427.